

Non-topographic description of inherent structure dynamics in glass formers

Ludovic Berthier^{1,2} and Juan P. Garrahan¹

¹*Theoretical Physics, University of Oxford, 1 Keble Road, Oxford, OX1 3NP, UK*

²*Laboratoire des Verres, Université Montpellier II, 34095 Montpellier, France*

(Dated: November 1, 2018)

We show that the dynamics between inherent structures in glass forming systems can be understood in purely dynamical terms, without any reference to “topographic” features of the potential energy landscape. This “non-topographic” interpretation is based instead on the existence of dynamical heterogeneities and on their statistical properties. Our view is supported by the study of simple dynamically facilitated models of glass formers. These models also allow for the formulation of quantitative theoretical predictions which are successfully compared to published data obtained in numerical and experimental studies of local dynamics of supercooled liquids.

PACS numbers: 64.70.Pf, 05.50.+q

It's been like a kind of capsule, a bubble in time and space...

D. Lodge, *Paradise News*

I. INTRODUCTION

In 1969, Goldstein suggested that the dynamical slowdown of a liquid approaching its glass transition could be understood in terms of its potential energy landscape [1]. The practical implementation of this description was later introduced by Stillinger and Weber via the inherent structure (IS) formalism [2]. The landscape or “topographic” view has become one of the paradigms in the field [3, 4]. The purpose of this paper is to pursue, however, the rather orthogonal idea that the landscape description is essentially incomplete, in the sense that from the statistical properties of IS, or similar static characteristics, it is not possible to capture the central spatial and dynamical aspects of the physics of glass formers. Instead, we aim here at a “non-topographic” reinterpretation of the dynamics between IS, showing that the central role is played by dynamical heterogeneities, without resorting to any special features of the potential energy landscape.

The connection between the existence of a dynamical correlation length and the landscape description is in fact implicitly present in the original papers [1, 5], although it only clearly appears in more recent works [6, 7, 8, 9, 10]. The connection relies on two remarks. (i) According to Goldstein [1], the landscape is useful for “viscous” liquids, for which a separation of time scales between fast vibrations and slower structural relaxations exists. This gives rise to the notions of “basins” or “traps” which are then purely dynamical concepts. (ii) Escape from these traps was described to be “localized” in space [1], a fact which was later numerically confirmed [5]. The transition rate between basins therefore becomes extensive “for large enough systems” [5]. How large the system must be, what is the geometry, and what are the typical length and time scales of these rearrangements are crucial questions left unanswered unless spatial and dynamical aspects are included explicitly in the theoretical

description.

In what follows we show that natural answers can be obtained in the context of dynamical heterogeneities [11], thus leading to a consistent qualitative interpretation of IS dynamics. This we demonstrate using the simplest models which capture the phenomenon of dynamic heterogeneity, and for which the landscape properties are completely irrelevant (sections II and III). We also show that a satisfactory quantitative agreement with numerical and experimental studies of mesoscopic systems can be obtained (section IV), emphasizing the relevance of the non-topographic description of supercooled liquid dynamics discussed in this paper.

II. DYNAMICAL HETEROGENEITIES VERSUS “HIDDEN INHERENT STRUCTURES”

In a cold dense liquid mobility is sparse. A microscopic immobile region is mostly surrounded by other immobile regions. It can become mobile only if it is next to a rare microscopic mobile region: its dynamics is facilitated by the presence of an unjammed mobile neighbour. This is the concept of dynamic facilitation, originally introduced in [12], which leads to the phenomenon of dynamic heterogeneity [13, 14].

The elementary models which capture the idea of dynamic facilitation are the Fredrickson-Andersen (FA) [12] and the East [15] spin facilitated models (see [16] for a comprehensive review). They consist of a chain of two-state spins, $n_i = 0, 1$ ($i = 1 \dots N$), with non-interacting Hamiltonian $H = \sum_i n_i$, and single spin flip dynamics subject to local kinetic constraints. In the FA model, a spin can flip if either of its nearest neighbours is in the up state, while in the East model a spin can flip only if its nearest neighbour to the right is up. The equilibrium behaviour of both models is that of an ideal gas of binary excitations, with an equilibrium concentration of up spins given by $c = 1/(1 + e^{1/T})$ at temperature T . At low temperatures the dynamics is glassy due to the competition between decreasing the energy and the need for facilitating spins. The FA model is Arrhenius, or strong,

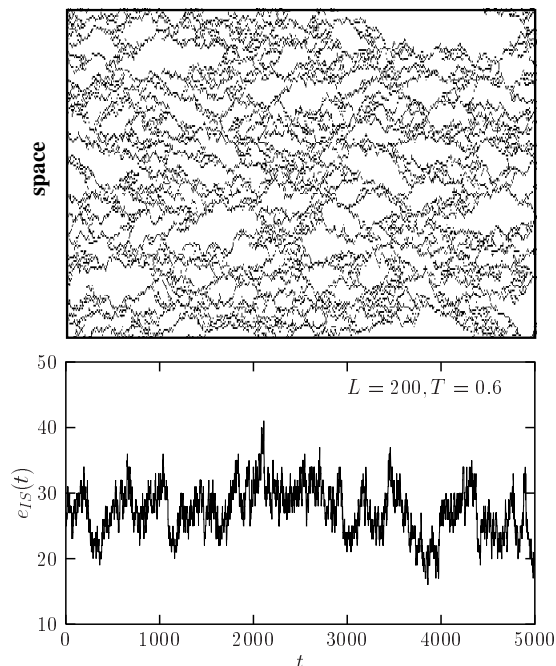


FIG. 1: Top: an IS trajectory in the FA model at $T = 0.6$ and system size $L = 200 = 32 \ell(T)$; vertical axis is space, horizontal one is time, up spins are black. Bottom: the corresponding time series of the IS energy.

in the jargon of supercooled liquids [17], with relaxation time $t_{\text{rel}} = e^{3/T}$. The East model is super-Arrhenius, or fragile, $t_{\text{rel}} = e^{1/(T^2 \ln 2)}$.

In order to study the dynamics of IS in the FA and East models we consider the single spin Monte Carlo dynamics in equilibrium at temperature T , using a combination of Metropolis and continuous time algorithms [18]. At each Monte Carlo step, we quench the system by running a zero temperature Metropolis dynamics. We thus obtain the finite T and its corresponding IS trajectory, as initially suggested in the context of liquids. In Fig. 1 (top), we show such an IS trajectory in the FA model at $T = 0.6$. The vertical axis corresponds to space and the horizontal one to time. Up (down) spins in the IS configuration are denoted black (white). The IS structure trajectory is very close to that of the corresponding finite T one. This is due to the fact that, as a consequence of the kinetic constraints, an up spin can be relaxed under the quench only if a neighbour is in the up state, so that the quenching procedure does not break the continuity of the up spin “world-lines”. This IS trajectory then displays the structure of a dense mixture of “bubbles” separated by excitation lines, as discussed in [14]. In Fig. 1 (bottom), we show the evolution of e_{IS} , the (extensive) energy of the IS, as a function of time t . The time series is featureless, corresponding to a sequence of many uncorrelated events. This is analogous to what is found in simulations of liquids for high temperatures or

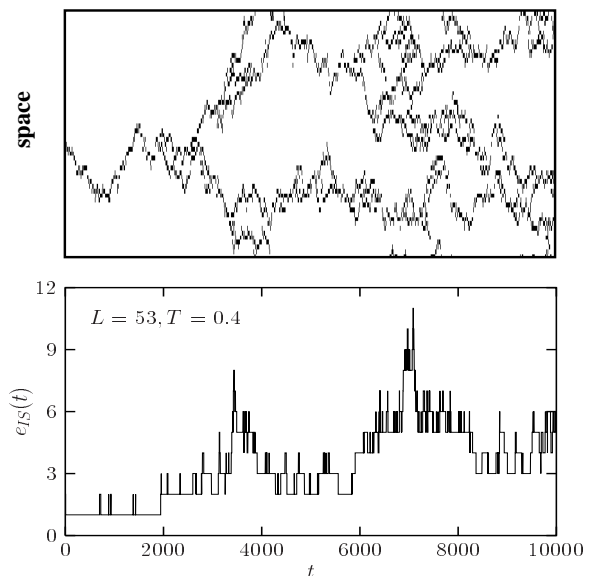


FIG. 2: Same as Fig. 1 but for $T = 0.4$ and $L = 53 = 4 \ell(T)$.

large system sizes [7, 19].

The existence of a dynamical coherence length, $\ell(T)$, is however clear from the IS trajectory in Fig. 1. Individual transitions in IS correspond to the birth or closure of the trajectory space bubbles, i.e., the branching or coalescence of excitation lines. The dynamical correlation length $\ell(T)$ is thus given by the typical size of the bubbles, which is fixed by the equilibrium concentration of excitations, $\ell(T) = c^{-1}(T)$. In Fig. 1, the system size L is much larger than $\ell(T)$, $L = 32 \ell(T)$. In Fig. 2 we show instead an IS trajectory and its corresponding e_{IS} time series in a case where the system size is much closer to the coherence length, $L = 4 \ell(T)$. The time series for e_{IS} now displays the coherent changes in IS energies also observed in numerical simulations of “sufficiently small” supercooled liquids [7, 8, 19]. Obviously, “sufficiently small” only becomes a well-defined statement when $\ell(T)$ is first defined. We emphasize also that these “hidden structures” follow here from the presence of dynamical heterogeneities, with no obvious relation to specific topographic features of the energy landscape, which in this case is trivial.

All the features of the e_{IS} time series in Fig. 2 (bottom) can be traced back to the slow bubbles, i.e., dynamic heterogeneities, in the trajectory of Fig. 2 (top). The fast spikes in Fig. 2 (bottom) correspond to smaller bubbles that “wet” the larger ones, which in turn determine the more persistent plateaus in e_{IS} . In principle one could renormalize out the smaller bubbles and obtain a time series for “metabasins” in analogy with [7, 8, 9]. In our case this is unnecessary since we know the space time distribution of bubbles [14] and we can therefore account for the effect in the IS dynamics of the whole range of dynamical heterogeneities. This is especially important in the case of the East model, where the hierarchical na-

ture of the dynamics leads to a fractal wetting structure which in turn is responsible for the temperature dependent stretching of correlation functions characteristic of fragile systems [14, 20].

III. LIFETIME OF HETEROGENEITIES VERSUS “HOPPING TIMES”

Each event in the time series of e_{IS} of Figs. 1 and 2 which increases/decreases the energy of the IS corresponds to the birth/closure of a bubble in trajectory space. The distribution of time intervals between events is then given by the distribution of time extensions of bubbles, or lifetimes of dynamical heterogeneities, $p(t)$. One has [14]:

$$p(t) = \int_0^\infty \rho(\ell)\rho(t|\ell)d\ell = \frac{t^{\beta-1}}{t_{\text{rel}}^\beta \mathcal{N}(\beta)} e^{-(t/t_{\text{rel}})^\beta}, \quad (1)$$

where $\rho(\ell) = c e^{-c\ell}$ is the distribution of length scales of heterogeneities, $\rho(t|\ell)$ the conditional distribution of corresponding time scales, and \mathcal{N} a normalization factor. The stretching exponent β is temperature independent, $\beta = 1/2$, for the FA model, and decreases with T for the East model, with $\beta \propto T$ at low temperatures. The correlation functions are determined through the persistence function $P(t) = \int_t^\infty p(t')dt' \simeq \exp[-(t/t_{\text{rel}})^\beta]$. These models are an explicit realization of stretched relaxation induced by the distribution of time and length scales of heterogeneous regions [11].

To numerically access the distribution (1), we follow the empirical procedure of Refs. [6, 7]. As for these simulations of supercooled liquids, we strike a compromise between small enough system sizes, comparable to the dynamic correlation length in order to distinguish between individual events, with large enough ones to avoid finite size effects, corresponding here to an upper cutoff of the integral (1). Again, the procedure becomes well-defined when $\rho(\ell)$ has first been defined, Eq. (1). In practical terms, we seek the smallest system size for which autocorrelation functions converge to those of the bulk. In the case of the FA and East models we have checked that this is obtained for systems of length $L \simeq 4\ell(T)$ and $8\ell(T)$, respectively. The difference stems from the hierarchical structure of time scales of the East model which enhances the relevance of larger length scales with respect to the FA case.

Figs. 3 and 4 show that Eq. (1) indeed describes the distribution of times between events—or “hopping times” in the language of [8, 9]—in the IS time series. Fig. 3 (top) presents for the FA model, at various low temperatures for system sizes $L = 4\ell(T)$, the IS energy correlation function, $C(t) = [\langle e_{IS}(t)e_{IS}(0) \rangle - \langle e_{IS}^2 \rangle]/L$. An almost temperature independent stretching, close to $\beta = 1/2$, is obtained, as expected at low temperatures, Eq. (1). In the lower panel of Fig. 3 we show the distribution of the logarithm of hopping times, $\pi(\ln t)$, for

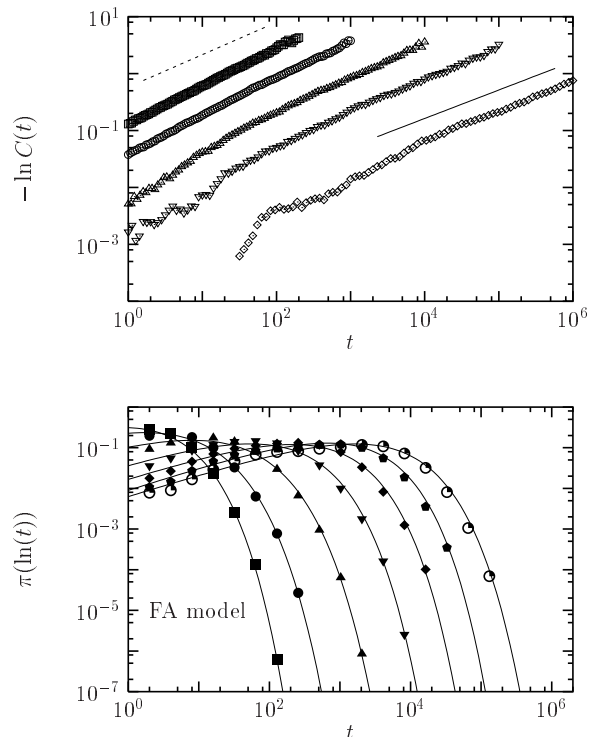


FIG. 3: Top: IS energy correlation function $C(t)$ for the FA model at various $T = 1.0, 0.6, 0.4, 0.3$ and 0.2 (from left to right) and system sizes $L = 4\ell(T)$, in a log-double log scale. The lines indicate stretching exponents $\beta = 0.57$ and $\beta = 0.5$ (from left to right). Bottom: distribution of hopping times; symbols correspond to simulation data at temperatures $T = 1.0, 0.6, 0.4, 0.3, 0.25, 0.22, 0.2$ (from left to right), and lines to fits using Eq. (1) with fixed $\beta = 1/2$.

a similar range of temperature and similar sizes. From Eq. (1), we have

$$\pi(\ln t) = \frac{1}{\mathcal{N}(\beta)} \left(\frac{t}{t_{\text{rel}}} \right)^\beta \exp \left[- \left(\frac{t}{t_{\text{rel}}} \right)^\beta \right]. \quad (2)$$

Symbols in the bottom panel of Fig. 3 indicate simulation data, while lines correspond to fits using Eq. (2) with $\beta = 1/2$, i.e., the single fitting parameter is the relaxation time $t_{\text{rel}}(T)$. The fits are excellent over several orders of magnitude. Fig. 4 presents a similar analysis for the East model, for systems sizes $L = 8\ell(T)$. The top panel shows $C(t)$. The temperature dependence of the stretching is obvious, and follows well the theoretical expectations. The bottom panel gives the data for hopping time distributions, and fits using Eq. (2), where now $\beta(T)$ is fixed from the corresponding values for $C(t)$. Again, the fits are good over several orders of magnitude.

The agreement between theory and simulations does not come as a surprise. This step was necessary, however, to establish the actual link between the dynamically heterogeneous dynamics of the system and the distribution

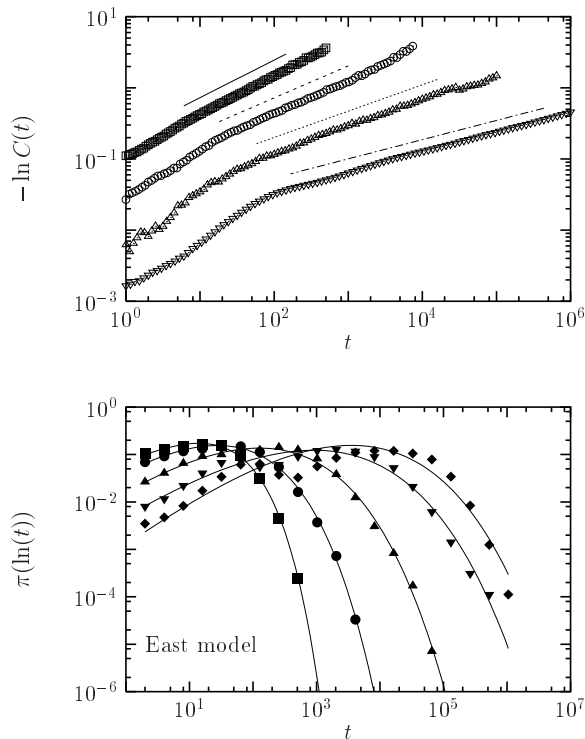


FIG. 4: Same as Fig. 3 but for East model. Top: Temperatures are $T = 1.0, 0.6, 0.4, 0.3$ (from left to right), and the stretching exponents are $\beta = 0.55, 0.45, 0.37$ and 0.27 (from left to right). Bottom: Temperatures are $T = 1.0, 0.6, 0.4, 0.3, 0.25$ (from left to right), the fits are from Eq. (2) with β fixed by the correlators.

of “hopping” or “trapping” times as measured in Refs. [8, 9, 10]. It also shows that these names (hopping, trapping) somehow obscure the physical interpretation.

IV. COMPARISON TO SIMULATIONS AND EXPERIMENTS

The spin facilitated models studied above are a simple instance where the phenomenon of dynamical “trapping” occurs due to the presence of spatial dynamical heterogeneities. Moreover, they are simple enough that the statistical properties of the “traps” can be worked out analytically. The basic initial observation of Stillinger and Weber was precisely the presence of these “hidden structures in liquid” [2, 19]. More recently, quantitative studies of the statistical properties of the IS dynamics in liquids have appeared [8, 9, 10]. The purely topographic interpretation of the data made in Refs. [8, 9, 10] was the main motivation for the current paper, since we think that the “basins”, “metabasins” or “traps” described in these works are a manifestation of the presence of dynamical heterogeneities, but not necessarily of static “traps”, as discussed in the previous sections.

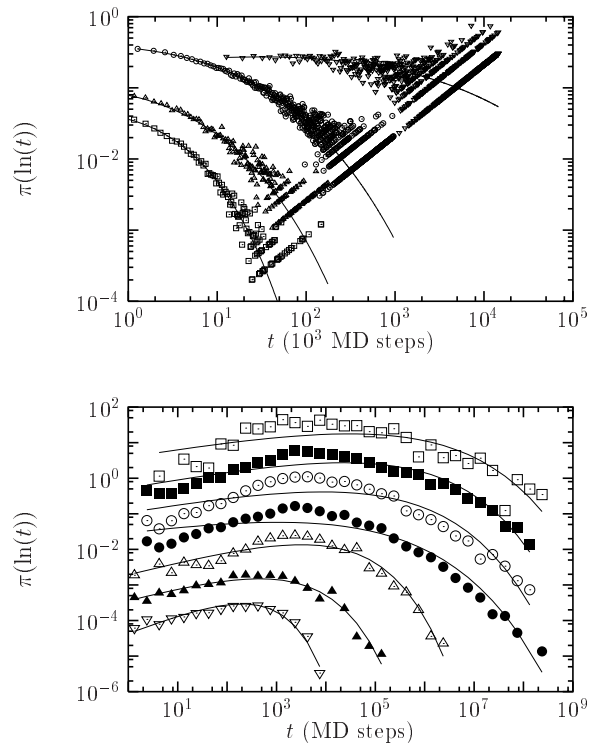


FIG. 5: Fits of LJ data from [8] (top) and [9] (bottom) using Eq. (2). The points are the published data, while the full lines are the fits, using two fitting parameters, β and t_{rel} at each T . Top: $(T, \beta, t_{\text{rel}})$ are $(0.49, 0.225, 30641)$ $(0.575, 0.275, 272)$ $(0.669, 0.316, 257)$ $(0.764, 0.428, 135)$ from top to bottom. Bottom: $(0.4, 0.234, 29500)$, $(0.435, 0.254, 24200)$, $(0.466, 0.246, 8820)$, $(0.5, 0.210, 1268)$, $(0.6, 0.358, 3138)$, $(0.8, 0.380, 452)$, $(1.0, 0.589, 203)$ from top to bottom.

Having theoretical predictions from the spin facilitated models, it is tempting to reanalyze published data to check whether predictions are able to describe also more realistic models and experiments. Our ambition here is not to claim that one-dimensional spin models are enough to describe the physics of three-dimensional molecular supercooled liquids, but rather to show that the mechanism described above is a simple and robust one, with an applicability well beyond these simple models [21].

In Fig. 5, we present the data for hopping time distributions from the simulations of [8] (top) and [9] (bottom). The lines through the symbols are fits using the distribution for dynamical heterogeneities log times of the FA/East models, Eq. (2). Apart from an irrelevant normalization constant, there are only two fitting parameters, the stretching exponent β and the relaxation time t_{rel} . The fits to the data of Denny et al. (top) are as good or better than those with a log normal distribution, as predicted by an activated scaling [8]. The agreement is also very good for Doliwa and Heuer’s data (bottom), which we have chosen to present as $\pi(\ln t)$ rather than as $p(t)$ as they were originally published in [9]. The de-

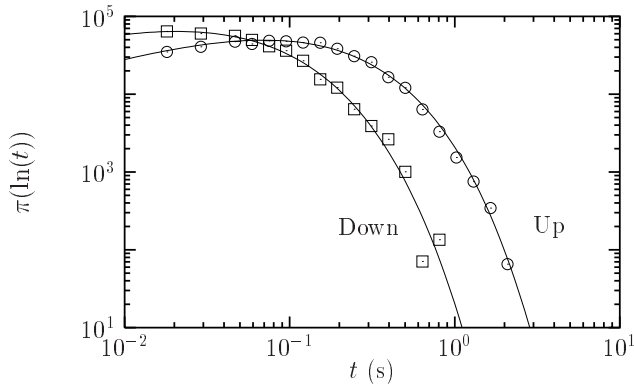


FIG. 6: Distributions of molecular switching times in polyvinyl acetate at 299 K, from Ref. [23], and fits using Eq. (2) with $\beta = 0.67$, $t_{\text{rel}} = 0.070$ s (Up), and $\beta = 0.63$, $t_{\text{rel}} = 0.021$ s (Down).

viations in the fits in this case are a consequence of the data for the very short times investigated in [9], where we expect the mechanism of dynamical facilitation to be less relevant, so that Eq. (2) should describe the tails of the distributions more accurately than the small times [22].

Finally, we have compared Eq. (2) to experimental observations. Although changing the system size is not conveniently realized in experiments, it is still possible to investigate the dynamics in “mesoscopic” regions, i.e., regions of a size comparable to the dynamic coherence length $\ell(T)$. In Ref. [23], time series for molecular polarization were obtained by Vidal Russell and Israeloff in local probe experiments on polyvinyl acetate films. Typical length scales probed through the use of non-contact atomic force microscopy techniques are $\simeq 20$ nm, i.e., not very large compared to the estimated size of heterogeneities [11]. Fortunately, since the polarization signal oscillates between two or four discrete levels, fast thermal fluctuations only produce oscillations about these discrete values, so that the corresponding distributions for switching times can directly be compared to Eq. (2), therefore bypassing the IS construction.

We reproduce in Fig. 6 the distributions presented in the Fig. 5 of Ref. [23], where we have adopted a log scale for the time axis, and represented $\pi(\ln t)$ instead of $p(t)$, so that the comparison with the theoretical prediction (2) can be made on the entire range of time scales and also to facilitate the comparison with the results presented above. Again, we obtain an excellent fit of the experimental data to Eq. (2) for the complete experimental time window. The stretching exponents we find, $\beta = 0.67$ and 0.63 for the up and down polarizations, respectively, are slightly larger than the ones estimated in [23]. This is because the latter stemmed from a fit to a stretched exponential form of the tail of the distribution. Instead, it is clear from Fig. 6 that the power law prefactor is necessary to account for the whole spectrum

of time scales, and this shifts the stretching exponent to a slightly larger value.

V. CONCLUSIONS

We have shown that a consistent interpretation of the IS dynamics can be obtained solely invoking spatial and dynamical aspects related to the statistical properties of the dynamic heterogeneity of supercooled liquids. This physical picture was made more precise in the study of two simple dynamically facilitated spin models, which also allowed to obtain quantitative predictions which compare well to numerical and experimental data. Our results are additional evidence that dynamical heterogeneities play a crucial role in the physics of liquids approaching their glass transition [11].

In the topographic language, the so-called “landscape-influenced” regime evidenced by a decrease of $\langle e_{IS} \rangle$ with decreasing temperature is the relevant one in numerical simulations [3, 24]. In our non-topographic perspective, this decrease of the IS energy corresponds to a decreasing concentration of facilitating defects [21], i.e., to the growth of the dynamical coherence length which is in turn directly responsible for the dynamical slowdown. It is therefore striking that the physics at relatively high temperatures, i.e., above the estimated mode-coupling temperature T_c , can be described by the same physical mechanism of dynamic facilitation initially supposed to be relevant close to the experimental glass transition T_g . Hence, our results imply that the dynamics above T_c is heterogeneous, in agreement with simulations [25].

Moreover, as suggested in [8, 9], it logically follows that the physics in this regime is qualitatively not very different from the one at temperatures closer to T_g . This is at odds with the common belief that a change of mechanism takes place close to T_c [4]. This raises two interesting questions that we formulate as a conclusion to the paper. First, in the language of heterogeneities, what is the meaning, if any, of the crossovers reported close to T_c ? Second, since these crossovers somehow justify the use of the mode-coupling theory above T_c , why does the theory apparently work in a regime where the dynamics is heterogenous, and why does it eventually break down at lower temperatures?

Acknowledgments

We are grateful to J.-P. Bouchaud, D. Chandler, D.R. Reichman and G. Tarjus for discussions. We thank the authors of Refs. [8, 9, 23] for kindly providing their published data. We acknowledge financial support from a European Marie Curie Fellowship No HPMF-CT-2002-01927, CNRS (France), Worcester College Oxford, EPSRC Grant No. GR/R83712/01, and the Glasstone Fund. Some of the numerical results were obtained on Oswell at the Oxford Supercomputing Center, Oxford University.

-
- [1] M. Goldstein, *J. Chem. Phys.* **51**, 3728 (1969).
- [2] F.H. Stillinger and T.A. Weber, *Phys. Rev. A* **25**, 978 (1982).
- [3] F.H. Stillinger, *Science* **267**, 1935 (1995).
- [4] P.G. Debenedetti and F.H. Stillinger, *Nature* **410**, 259 (2001).
- [5] F.H. Stillinger and T.A. Weber, *Science* **225**, 983 (1984).
- [6] S. Büchner and A. Heuer, *Phys. Rev. E* **60**, 6518 (1999).
- [7] S. Büchner and A. Heuer, *Phys. Rev. Lett.* **84**, 2168 (2000).
- [8] R.A. Denny, D.R. Reichman and J.-P. Bouchaud, *Phys. Rev. Lett.* **90**, 025503 (2003).
- [9] B. Doliwa and A. Heuer, *Phys. Rev. E* **67**, 030501 (2003).
- [10] B. Doliwa and A. Heuer, preprint cond-mat/0209139.
- [11] H. Sillescu, *J. Non-Cryst. Solids* **243**, 81 (1999); M.D. Ediger, *Annu. Rev. Phys. Chem.* **51**, 99 (2000).
- [12] G.H. Fredrickson and H.C. Andersen, *Phys. Rev. Lett.* **53**, 1244 (1984).
- [13] S. Butler and P. Harrowell, *J. Chem. Phys.* **95**, 4454 (1991).
- [14] J.P. Garrahan and D. Chandler, *Phys. Rev. Lett.* **89**, 035704 (2002).
- [15] J. Jäckle and S. Eisinger, *Z. Phys. B* **84**, 115 (1991).
- [16] F. Ritort and P. Sollich, cond-mat/0210382, to appear in *Adv. Phys.*
- [17] C.A. Angell, *Science* **267**, 1924 (1995).
- [18] M.E.J. Newman and G.T. Barkema, *Monte Carlo Methods in Statistical Physics*, (OUP, Oxford, 1999).
- [19] F.H. Stillinger and T.A. Weber, *Phys. Rev. A* **28**, 2408 (1983).
- [20] A. Buhot and J.P. Garrahan, *Phys. Rev. E* **64**, 021505 (2001).
- [21] J.P. Garrahan and D. Chandler, cond-mat/0301287.
- [22] We have checked that by making the exponent in the prefactor of (2) independent of β , thus allowing for an extra fitting parameter, we get excellent fits to the data. We have chosen not to present these fits, since our aim is less to propose a fit of numerical results than to discuss their physical interpretation.
- [23] E. Vidal Russell and N.E. Israeloff, *Nature* **408**, 695 (2000).
- [24] S. Sastry, P.G. Debenedetti, and F.H. Stillinger, *Nature* **393**, 554 (1998).
- [25] S. C. Glotzer, *J. Non-Cryst. Solids* **274**, 342 (2000).